Pergamon

Geochimica et Cosmochimica Acta, Vol. 60, No. 24, pp. 5037–5043, 1996

0016-7037/96 $15.00 + .00

PII S0016-7037(96)00293-1

Strontium diffusion in sanidine and albite, and general comments on strontium diffusion in alkali feldspars

D. J. CHERNIAK

Department of Earth and Environmental Sciences, Rensselaer Polytechnic Institute, Troy, NY 12180-3590, USA

(*Received January* 5, 1996; *accepted in revised form August* 19, 1996)

Abstract—Strontium chemical diffusion has been measured in albite and sanidine under dry, 1 atm, and QFM buffered conditions. Strontium oxide-aluminosilicate powdered sources were used to introduce the diffusant and Rutherford Backscattering Spectroscopy (RBS) used to measure diffusion profiles. For the 1 atm experiments, the following Arrhenius relations were obtained:

Sanidine (Or_{61}), temperature range 725–1075°C, diffusion normal to (001):
$D = 8.4 \exp(-450 \pm 13 \text{ kJ mol}^{-1}/RT) \text{ m}^2\text{s}^{-1}$.

Albite (Or_1), temperature range 675–1025°C, diffusion normal to (001):
$D = 2.9 \times 10^{-9} \exp(-224 \pm 11 \text{ kJ mol}^{-1}/RT) \text{ m}^2\text{s}^{-1}$.

The alkali feldspars in this and earlier work display a broad range of activation energies for Sr diffusion, which may be a consequence of the thermodynamic non-ideality of the alkali feldspar system and/or the mixed alkali effect.

1. INTRODUCTION

This paper is a continuation of earlier work on Sr diffusion in feldspars (i.e., Cherniak and Watson, 1992, 1994), using much the same experimental approach. As we have previously noted, Sr diffusion rates are clearly important in the interpretation of Rb-Sr isotope ratio measurements. The feldspars, because of their abundance in crustal rocks and their ability to incorporate Rb and Sr into their structures, play a dominant role in the isotope systematics of the Rb-Sr system.

This work is also a summary of sorts, and an attempt to discover any systematic trends in the existing data on Sr diffusion in alkali feldspars. In the process, we attempt to better understand the influence of the chemical and structural characteristics of feldspars on Sr diffusion.

2. EXPERIMENTAL PROCEDURE

The feldspars used in this study were sanidine (Or_{61}) from Sri Lanka (kindly provided by Don Miller) and albite (Or_1) from Brazil (#135031) from the collection at the National Museum of Natural History. Compositional information obtained from electron microprobe analysis of the feldspars is presented in Table 1.

The specimens used in experiments were glass-clear and free of obvious inclusions. Samples for (001) and (010) orientations of sanidine and (001) orientation of albite were prepared by cleaving the feldspar along these planes and cutting cleaved slabs into pieces a few millimeters square with a low-speed wafering saw. Samples for experiments to be run in air were pre-annealed at 1000°C for 48 h in air, mainly to assess the thermal stability of specimens. Those to be run under QFM conditions were pre-annealed in sealed silica capsules with a solid buffer for similar times and temperatures. Annealing samples prior to the diffusion experiments also provides some constraints on initial defect chemistry, and should bring the feldspars into similar states of Al-Si order (e.g., Brown and Parsons, 1989). Given the time-temperature conditions of the diffusion anneals, further significant changes in Al-Si order beyond that achieved in the pre-annealing step are unlikely. The duration of the pre-anneals may be insufficient to attain complete disordering if the process occurs only through Al-Si diffusive exchange, which is likely the case for anhydrous, 1 atm conditions (Brown and Parsons, 1989; Goldsmith and Jenkins, 1985; Grove et al., 1984). Although we cannot precisely characterize the state of Al-Si order in the feldspars before and after the various annealing steps, it is not necessarily a factor that will have a significant influence on diffusion (Yund, 1983).

Experiments annealed in air were conducted in a manner similar to that described in our earlier Sr diffusion studies (Cherniak and Watson, 1992, 1994). The source material used was a mixture of SrO, Al_2O_3, and SiO_2 powders. Diffusion experiments using the QFM buffer were conducted as follows: the source of diffusant was a combination of a Sr-aluminosilicate powder (oxides combined in appropriate proportions to obtain $SrAl_2Si_2O_8$) and alkali feldspar of the same composition as the feldspar sample (i.e., Or_{61} or Or_1). Source components were fused at 1200°C and ground to fine powders under alcohol. Samples (pre-annealed under QFM conditions as noted above) were placed in Pt capsules with the source material and sealed in silica glass tubes under vacuum with a solid buffer. Both sources experienced some sintering during the diffusion anneals but were generally readily removed from the sample surfaces (Fig. 1).

Following diffusion anneals, samples were removed from capsules, rinsed briefly in dilute HCl, and ultrasonically cleaned in distilled water and ethanol to remove residual source material clinging to sample in preparation for RBS analysis. In a few cases, residual source material could not be completely removed so that there was sufficient clear surface area for analysis; these experiments were rerun.

3. RUTHERFORD BACKSCATTERING SPECTROSCOPY ANALYSIS

Strontium concentration profiles were measured with RBS (2 MeV He^+ beam). RBS analysis and data reduction approaches have been described in previous work (e.g., Cherniak and Watson, 1992, 1994; Cherniak and Ryerson, 1993), and will not be discussed in detail here. As in those studies, diffusion was modeled as transport in a semi-infinite medium with constant surface concentration (i.e., a complementary error function solution). Uncertainties in depth determination are constrained primarily by the resolution of the solid-state surface barrier detector used to acquire the backscattered helium ions. Depth resolution is about 10 nm in the near surface

Table 1. Representative electron microprobe analysis of feldspars used in this study.

	Sanidine	Albite
SiO_2	66.77	68.28
Al_2O_3	19.06	19.23
FeO	0.00	0.01
CaO	0.00	0.03
K_2O	10.54	0.22
Na_2O	4.50	11.63
total	100.04	99.40

region, but broadening somewhat at greater depths due to energy spread of the He ions as they travel through the sample. Uncertainties in Sr concentration are primarily controlled by counting statistics (i.e., error proportional to $\sqrt{N}$, where N is the number of counts in a segment of the Sr profile). Depth profile lengths ranged from several tens to several hundred nanometers. Strontium surface concentrations were on average ~0.5 mol%. Typical profiles and their inversion through the error function are shown in Fig. 2.

4. RESULTS

4.1. Sanidine

The results for sanidine are presented in Table 2 and plotted in Fig. 3. A least-squares fit to the data collected for the (001) orientation yields an activation energy of 450 ± 13 kJ mol^{-1} (108 kcal mol^{-1}) and pre-exponential factor 8.4 m^{2}s^{-1} (log D_0 = 0.9252 ± 0.5893). Results for both (010) orientation and QFM anneals (001) orientation were similar to those for (001) anneals in air.

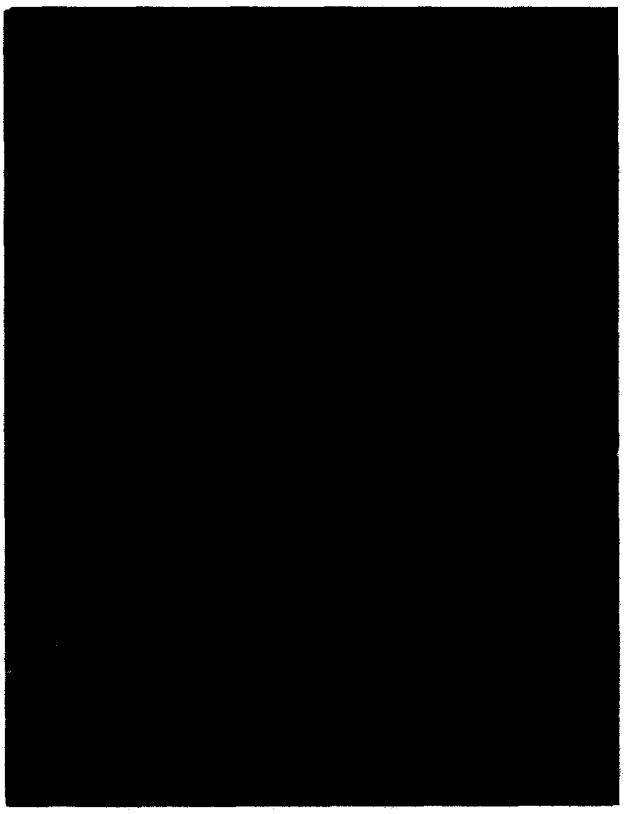

FIG. 1. SEM image of a feldspar surface following Sr diffusion anneal. Little of the source material generally adheres to sample surfaces.

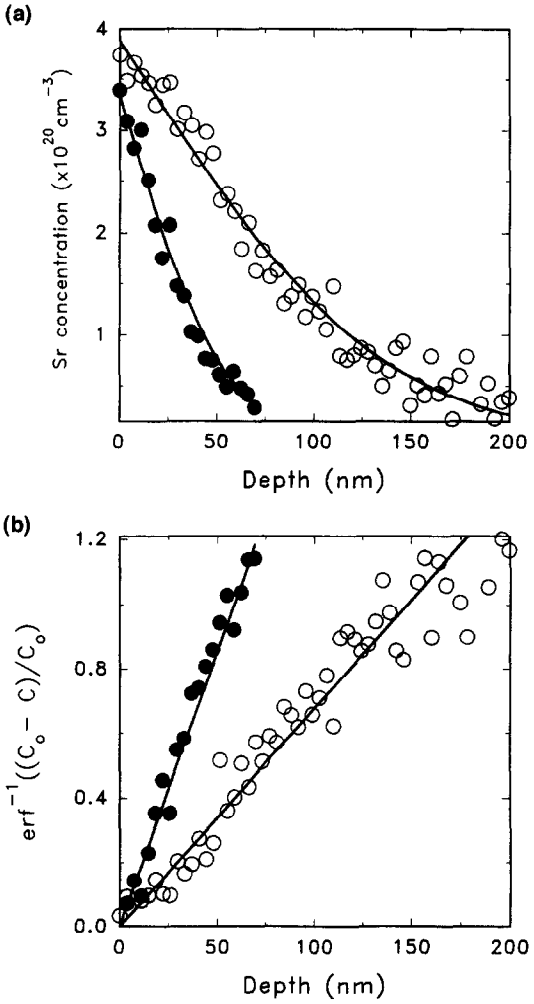

FIG. 2. Typical Sr diffusion profiles. (a) Profiles are plotted with complementary error function curves. (b) The data are linearized by inversion through the error function.

4.2. Albite

The Sr diffusion data for albite are plotted in Fig. 4 and presented in Table 3. A least-squares fit to the results for anneals in air yields the activation energy 224 ± 11 kJ mol^{-1} (54 kcal mol^{-1}) and pre-exponential factor 2.5 × 10^{-9} m^2 s^{-1} (log D_0 = −8.6040 ± 1.5606). In contrast to the sanidine, QFM results differ significantly from those for samples annealed in air. The activation energy for diffusion under buffered conditions is significantly larger (326 ± 35 kJ mol^{-1}, 78 kcal mol^{-1}); the pre-exponential factor is 2.7 × 10^{-5} m^2 s^{-1} (log D_0 = −4.5729 ± 1.5606).

4.3. Time Dependence of Diffusion

In order to determine whether lattice diffusion is the dominant process being measured, we undertook both a time-

Table 2. Diffusion Data for Sr in Sanidine (Or_{61}).

sample	T (°C)	t (sec)	D(m^2sec^{-1})	log D	(+/-)
Diffusion normal to (001):					
AOSr-17	725	$7.95x10^6$	$6.33x10^{-23}$	-22.20	0.30
AOSr-2	775	$3.10x10^6$	$3.71x10^{-22}$	-21.43	0.13
AOSr-13	825	$1.29x10^6$	$2.56x10^{-21}$	-20.59	0.10
AOSr-6	875	$2.70x10^5$	$3.24x10^{-20}$	-19.49	0.06
AOSr-1	925	$8.70x10^4$	$3.45x10^{-19}$	-18.46	0.09
AOSr-3	925	$6.08x10^5$	$2.21x10^{-19}$	-18.66	0.19
AOSr-12	925	$5.07x10^5$	$8.58x10^{-20}$	-19.07	0.17
AOSr-5	925	$1.82x10^5$	$1.60x10^{-19}$	-18.97	0.12
AOSr-11	925	$8.28x10^4$	$1.12x10^{-19}$	-18.95	0.05
AOSr-4	925	$5.10x10^4$	$1.53x10^{-19}$	-18.82	0.05
AOSr-7	925	$2.16x10^4$	$1.07x10^{-19}$	-18.97	0.16
AOSr-14	975	$3.24x10^4$	$2.22x10^{-18}$	-17.65	0.02
AOSr-8	975	$2.72x10^4$	$2.43x10^{-18}$	-17.61	0.12
AOSr-15	1025	$2.70x10^3$	$6.15x10^{-18}$	-17.21	0.03
AOSr-10	1075	$5.10x10^3$	$6.03x10^{-17}$	-16.22	0.09
Diffusion normal to (010):					
AOSr-21	825	$1.52x10^6$	$2.25x10^{-21}$	-20.65	0.09
AOSr-20	925	$1.89x10^5$	$4.42x10^{-19}$	-18.35	0.04
AOSr-22	975	$3.24x10^4$	$2.28x10^{-18}$	-17.64	0.05
QFM Buffer (normal to (001)):					
AOSr-23	825	$1.11x10^6$	$2.44x10^{-21}$	-20.61	0.12
AOSr-25	875	$8.52x10^4$	$4.74x10^{-20}$	-19.32	0.13
AOSr-26	925	$2.16x10^4$	$1.12x10^{-19}$	-18.95	0.10
AOSr-27	925	$8.64x10^4$	$9.93x10^{-20}$	-19.00	0.11

series study and zero-time experiments for each feldspar composition. Figure 5 shows the results of the time-series study. Although there is some scatter in the sanidine results, diffusivities are relatively constant over times differing by over an order of magnitude. Diffusion coefficients for albite for diffusion times differing by a factor of 5 agree within error. The zero-time experiments (not plotted) show little uptake of Sr in short anneals (essentially the few minutes required to heat samples to 925°C and quench) for either albite or sanidine.

5. DISCUSSION

Since we have Sr diffusion data for other alkali feldspar compositions, we can compare the findings from the present study with them. These data are compared in Fig. 6. The QFM data reported in this work will not be discussed further; these results will be considered in detail elsewhere (D. J. Cherniak and E. B. Watson, unpubl. data). Unlike plagioclase, in which activation energies for Sr diffusion are quite similar (although diffusivities vary markedly with An content; cf. Cherniak and Watson, 1994; Giletti and Casserly, 1994), the alkali feldspars have quite different activation energies for Sr diffusion in air but generally comparable diffusivities over the investigated temperature range.

While there is a good deal of diffusion data for near endmember alkali feldspars, there exist little for intermediate compositions. Christofferson et al. (1983) and Brady and Yund (1983) have investigated Na-K interdiffusion in alkali feldspars and found that interdiffusion rates are strongly influenced by composition. Alkali feldspars of intermediate Or content (i.e., $\sim Or_{20}$ to Or_{60}) have lower interdiffusion coefficients than those nearer endmember compositions at both 1000 and 900°C (Christofferson et al., 1983). This observed behavior is largely a result of the non-ideality of alkali feldspar solid solution. Activation energies for K-Na interdiffusion are also expected to be influenced by composition based on calculations using self-diffusion data and thermodynamic mixing parameters (e.g., Christofferson et al., 1983). Strontium chemical diffusion in alkali feldspars could be similarly affected by non-ideality, especially since Sr exchange likely occurs through a vacancy process and depends

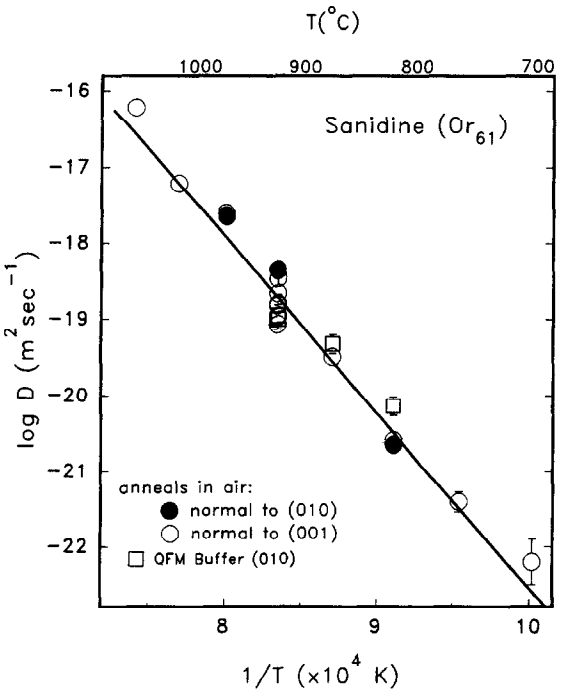

FIG. 3. Arrhenius plot for Sr diffusion in sanidine, showing results for anneals in air of (001) and (010) orientations, and anneals under QFM buffered conditions. The line is a least-squares fit to the (001) data, which yields an activation energy of 450 kJ mol^{-1} and pre-exponential factor 8.4 m^2s^{-1}.

on the movement of both Na and K, whose lattice sites it occupies.

In Fig. 7, Sr diffusion coefficients for a number of temperatures are plotted as a function of Or content to bring out any systematic behavior. While diffusivities at high temperatures are relatively insensitive to composition, a pronounced curvature develops in the relationship at lower temperatures, with diffusivities for intermediate compositions slower than those of near endmembers. These trends roughly correspond to that observed by Christofferson et al. (1983) (also plotted in Fig. 7), although the minima of our distribution appears to be skewed a bit toward higher Or content. Admittedly, the lowest temperature points are based on extrapolation (and the extrapolations themselves may come into question because the Arrhenius relationships may not hold at lower temperature due to the non-ideality of the system) but the trend of lower D for intermediate Or content does appear in the temperature range of the experiments (although it is not nearly as pronounced as at lower temperature).

The situation for Sr is also complicated by several additional factors beyond the thermodynamic non-ideality of the alkali feldspar matrix. The ionic radius of Sr is approximately midway between K and Na, and thus Sr does not have a comfortable "fit" in lattice sites when exchanging with either of these cations (as would Ca for Na and Ba for K). In addition, its nonequivalent charge (i.e., +2 vs. +1 for the alkalis) requires a charge compensating species to maintain electrical neutrality. These factors are likely to influence Sr diffusion, as they also apparently account for the nonsystematic partitioning behavior of Sr in alkali feldspars. On a first-order basis, however, it appears that Sr chemical diffusion is influenced by composition in a manner similar to K-Na interdiffusion.

We considered several approaches to modeling the alkali-Sr exchange, but could not come up with any satisfactory means given the limited availability of information. The system is actually a ternary (or even a 4- or 5-component system if one considers possible charge-compensating species). While thermodynamic parameters exist for Sr-Na, Sr-K, and K-Na binaries in feldspars (e.g., Kotelnikov and Chernysheva, 1995), those in more complex systems are difficult to quantify. Other necessary parameters, such as the dependence of tracer diffusivities on feldspar composition, have not been directly evaluated. It should also be noted that even in the much simpler system of alkali interdiffusion investigated by Christofferson et al. (1983), agreement between the interdiffusion model and the data was limited. The model predicted the general shape of the curves (diffusivity as a function of Or content) but the calculated diffusivities themselves agreed poorly with the measured results. In addition, other factors, such as those outlined below, may influence Sr mobility.

5.1. The Mixed-Alkali Effect

An additional factor that may influence alkali feldspar diffusion behavior and account for some of the observed differences among these feldspars is the "mixed-alkali" effect. Briefly, the mixed alkali effect involves a change in

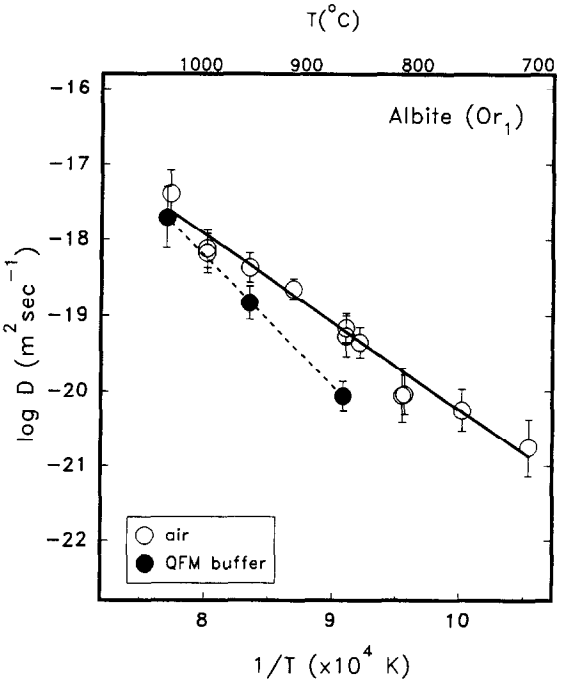

FIG. 4. Arrhenius plot for Sr diffusion in albite ((001) orientation) comparing results for anneals in air with those run under buffered conditions. Least-squares fits to both datasets are plotted, activation energy and pre-exponential factor for Sr diffusion in air are 224 kJ mol^{-1} and 2.5×10^{-9} m^2s^{-1}, respectively; these parameters are 326 kJ mol^{-1} and 2.7×10^{-5} m^2s^{-1} for the QFM-buffered experiments.

Table 3. Diffusion Data for Sr in Albite (Or_1).

sample	T (°C)	t (sec)	D(m^2sec^{-1})	log D	(+/-)
Diffusion normal to (001):					
SrAb-7	676	$2.59x10^6$	$1.77x10^{-21}$	-20.75	0.38
SrAb-6	725	$1.47x10^6$	$5.65x10^{-21}$	-20.25	0.28
SrAb-16	775	$3.58x10^5$	$9.22x10^{-21}$	-20.04	0.26
SrAb-17	774	$5.33x10^5$	$8.97x10^{-21}$	-20.05	0.36
SrAb-3	812	$8.64x10^4$	$4.51x10^{-20}$	-19.35	0.20
SrAb-8	825	$1.17x10^5$	$6.91x10^{-20}$	-19.16	0.19
SrAb-11	825	$6.23x10^5$	$5.31x10^{-20}$	-19.27	0.27
SrAb-18	878	$8.64x10^4$	$2.23x10^{-19}$	-18.65	0.14
SrAb-10	925	$1.20x10^4$	$4.31x10^{-19}$	-18.37	0.19
SrAb-12	975	$7.20x10^3$	$7.67x10^{-19}$	-18.12	0.25
SrAb-14	975	$1.17x10^4$	$6.65x10^{-19}$	-18.18	0.26
SrAb-13	1021	$1.80x10^3$	$4.13x10^{-18}$	-17.38	0.30
QFM Buffer (normal to (001)):					
SrAb-20	828	$1.08x10^5$	$8.77x10^{-21}$	-20.06	0.20
SrAb-19	925	$2.34x10^4$	$1.49x10^{-19}$	-18.83	0.22
SrAb-21	1026	$4.50x10^3$	$2.00x10^{-18}$	-17.70	0.41

various material properties (e.g., resistivity, viscosity, activation energies for kinetic processes) when two alkalis are included in the material as major constituents. The maximum deviations from endmember (i.e., one-alkali system) behavior occur at about a 50:50 ratio of alkalis (Day, 1976). The effect appears to be enhanced by increasing differences between the sizes of the respective alkalis, and tends to become less pronounced in systems with lower total alkali content (Hakim and Uhlmann, 1967). Although most commonly observed in glasses, it has been reported in crystalline materials as well (Day, 1976). The mixed alkali effect cannot be attributed to phase separation, and is observed even when there is no evidence of immiscibility or deviation from ideal solution behavior (Hakim and Uhlmann, 1967). While not yet well understood, the effect does appear to have a structural basis. EXAFS studies of $[K_xCs_{1-x}]_2Si_2O_5$ glasses (Greaves, 1990) and glasses made of mixtures of orthoclase and albite (Jackson et al., 1987) suggest that local structural environments of alkalis are influenced by the presence of the other alkali. Mobilities of alkalis will likely be limited because available sites are not "matched" to both alkalis, especially when they vary widely in size. The activation energy for transport of a particular alkali is also expected to increase as its concentration decreases and the surrounding sites are more influenced by the other alkali. Since both alkali components of the system are comparably influenced, the effect should be most pronounced at around a 50:50 ratio of the alkalis (Greaves, 1990). As noted above, Sr transport is likely to be influenced by alkali mobility since it occupies alkali sites in the feldspar lattice.

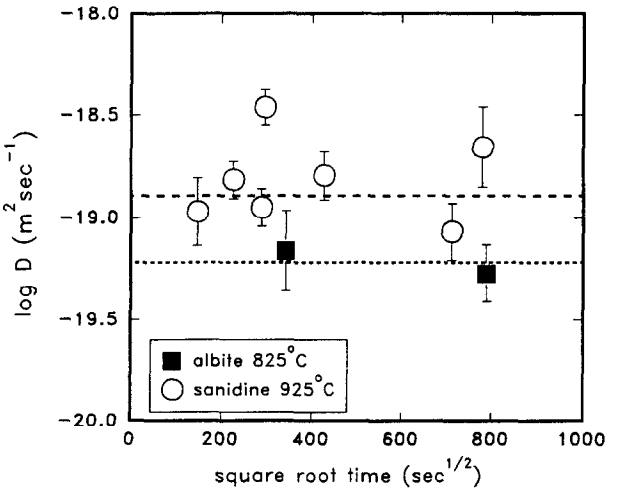

FIG. 5. Time dependence of diffusion anneals at fixed temperature, showing results for both albite and sanidine.

5.2. Geochemical Implications

The differences in Sr diffusion rates among the alkali feldspars may lead to significant variations in retentivity of strontium isotopes. To assess the magnitude of the effect of composition on geochemical behavior, we calculate closure temperatures for Sr, using the model of Dodson (1973) and the assumption of spherical geometry (i.e., geometric factor

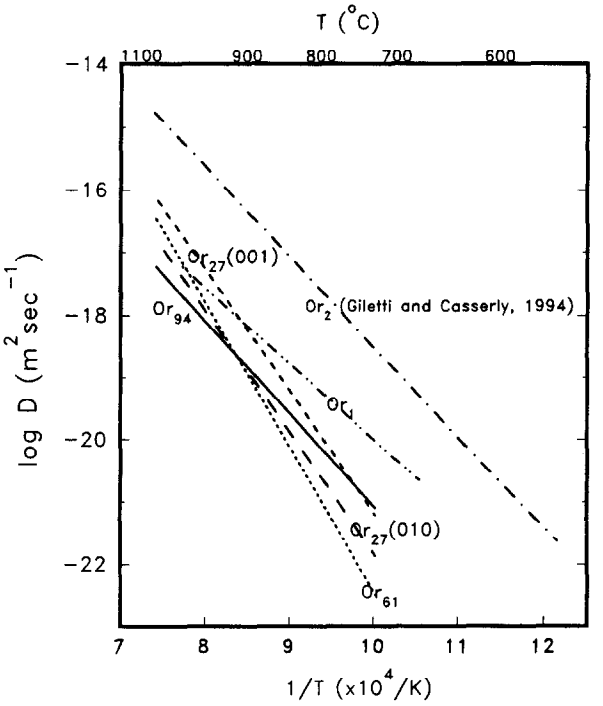

FIG. 6. Summary plot of Sr diffusion results for alkali feldspars annealed in air. It is clear that there is a wide variation in activation energies for Sr diffusion across the range of alkali feldspar compositions. Values for activation energies (in kJ mol^{-1}) are as follows: Or_1 – 231; Or_2 – 279; Or_{27} (001) – 373; Or_{27} (010) – 373; Or_{61} – 444; Or_{94} – 280. Data for orthoclase (Or_{94}) and anorthoclase (Or_{27}) are from Cherniak and Watson (1992).

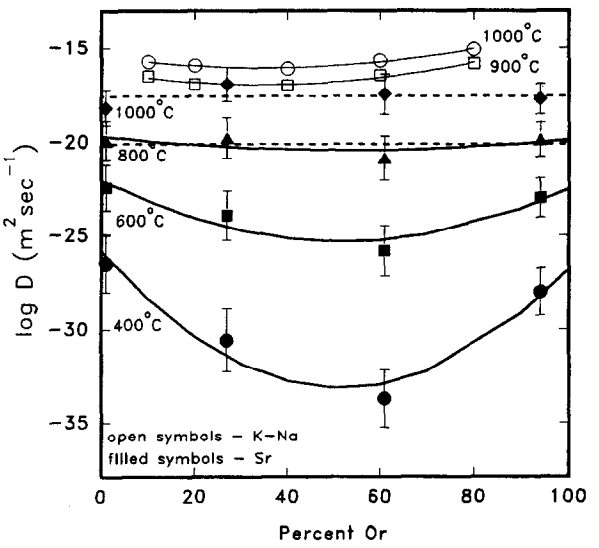

FIG. 7. Illustration of variation in diffusivities with Or content for both Sr diffusion and K-Na interdiffusion. Both data sets display a decrease in diffusivities for intermediate alkali feldspar compositions. The K-Na interdiffusion data are from Christofferson et al. (1983), the Sr data are from the present work and Cherniak and Watson (1992).

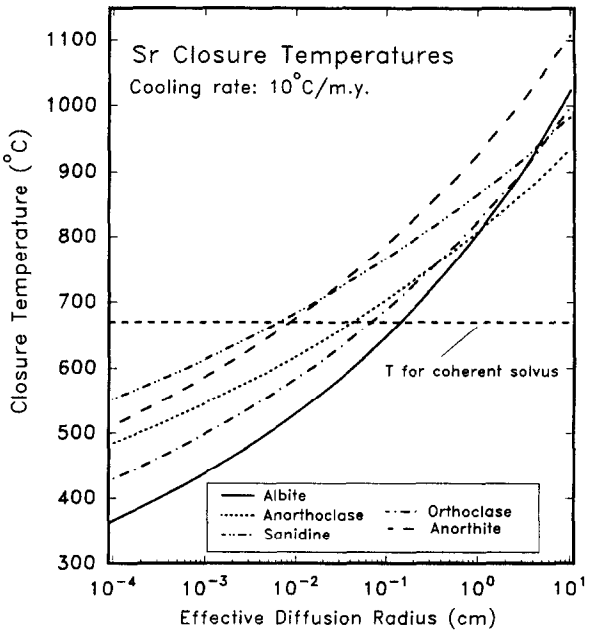

FIG. 8. Plot of closure temperatures for Sr in a range of feldspar compositions as a function of effective diffusion radius for a cooling rate of 10°C per million years. The horizontal line is the temperature for the coherent solvus. The intersection of this line with the closure temperature curves for intermediate alkali feldspars indicates critical ionic radii below which exsolution occurs before closure of the feldspar to Sr diffusion. For values of effective diffusion radius above these intersections, exsolution occurs after the feldspar is closed to Sr diffusion. Diffusion parameters used to calculate closure temperatures are from the present work and Cherniak and Watson (1992).

equal to 55). Closure temperatures are plotted in Fig. 8 as a function of effective diffusion radius.

The interpretation of, and indeed the significance of, closure temperatures in intermediate alkali feldspars are complicated by the occurrence of spinodal decomposition. For feldspars in the compositional range Or_{25}-Or_{45} with slow cooling rates, the position of the coherent solvus is ~670°C (Brown and Parsons, 1984). Given the shapes of solvus curves, this is also not an unreasonable estimate for the sanidine (Or_{61}). Thus, for cooling rates of 10°C/Ma, sanidines with effective diffusion radii greater than 60 μm will close to Sr diffusion before the onset of exsolution (Fig. 8). For the anorthoclase, this value is 400 μm. For smaller values, exsolution begins before the feldspar closes to Sr exchange. Since exsolution is largely rate-limited by alkali diffusion, it should proceed much more quickly than Sr diffusion. Given the complexity of the process, however, it is difficult to make general statements about the behavior and redistribution of Sr during exsolution.

If we consider conditions under which exsolution of the intermediate alkali feldspars has not yet occurred, Sr closure temperatures follow the trend $Or_{61} > Or_{27} > Or_{94} > Or_1$ for all but the largest effective diffusion radii. Because the diffusion parameters of the feldspars vary so widely, the relative differences between closure temperatures also change substantially with effective diffusion radius.

We can conclude, therefore, that intermediate composition

alkali feldspars generally have higher Sr closure temperatures (given a particular effective diffusion radius and temperatures above the onset of exsolution) than those nearer endmember compositions, but the relative differences between closure temperatures may vary significantly.

Acknowledgments—Feldspar specimens for this study were graciously provided by Paul Pohwat of the National Museum of Natural History and Don Miller. I thank Dave Wark for helpful discussion and some of the electron microprobe analyses. Constructive and insightful comments from R. A. Yund, T. L. Grove, and F. J. Ryerson helped significantly in improving the manuscript. This work was supported by grant EAR-9105055 from the National Science Foundation (to E. B. Watson). I especially thank Bruce Watson for his assistance throughout this project.

Editorial handling: F. J. Ryerson

REFERENCES

Brady J. B. and Yund R. A. (1983) Interdiffusion of K and Na in alkali feldspars: homogenization experiments. *Amer. Mineral.* **68,** 106–111.

Brown W. L. and Parsons I. (1984) Exsolution and coarsening mechanisms and kinetics in an ordered cryptoperthite series. *Contrib. Mineral. Petrol.* **86,** 3–18.

Brown W. L. and Parsons I. (1989) Alkali feldspars: Ordering rates, phase transformations and behaviour diagrams for igneous rocks. *Mineral. Mag.* **53,** 25–42.

Cherniak D. J. and Ryerson F. J. (1993) A study of strontium diffusion in apatite using Rutherford backscattering spectroscopy and ion implantation. *Geochim. Cosmochim. Acta* **57,** 4653–4662.

Cherniak D. J. and Watson E. B. (1992) A study of strontium diffusion in K-feldspar, Na-K feldspar and anorthite using Rutherford backscattering spectroscopy. *Earth Planet. Sci. Lett.* **113,** 411–425.

Cherniak D. J. and Watson E. B. (1994) A study of strontium diffusion in plagioclase using Rutherford backscattering spectroscopy. *Geochim. Cosmochim. Acta* **58,** 5179–5190.

Christofferson R., Yund R. A., and Tullis J. (1983) Inter-diffusion of K and Na in alkali feldspars: diffusion couple experiments. *Amer. Mineral.* **68,** 1126–1133.

Day D. E. (1976) Mixed alkali glasses—their properties and uses. *J. Non-Cryst. Solids* **21,** 343–372.

Dodson M. H. (1973) Closure temperature in cooling geochronological and petrological systems. *Contrib. Mineral. Petrol.* **40,** 259–274.

Giletti B. J. (1991) Rb and Sr diffusion in feldspars, with implications for cooling histories of rocks. *Geochim. Cosmochim. Acta* **55,** 1331–1343.

Giletti B. J. and Casserly J. E. D. (1994) Strontium diffusion kinetics in plagioclase feldspars. *Geochim. Cosmochim. Acta* **58,** 3785–3793.

Goldsmith J. R. and Jenkins D. M. (1985) The high-low albite relations revealed by reversal of degree of order at high pressures. *Amer. Mineral.* **70,** 911–923.

Greaves G. N. (1990) X-ray absorption spectroscopy. In *Glass Science and Technology* (ed. D. R. Uhlmann and N. J. Kreidl), Vol. 4B; *Advances in Structural Analysis,* pp. 1–76. Academic Press.

Grove T. L., Baker M. B., and Kinzler R. J. (1984) Coupled CaAl-NaSi diffusion in plagioclase feldspar: Experiments and applications to cooling rate speedometry. *Geochim. Cosmochim. Acta* **48,** 2113–2121.

Hakim R. M. and Uhlmann D. R. (1967) On the mixed alkali effect in glasses. *Phys. Chem. Glasses* **8,** 174–177.

Jackson W. E., Brown G. E., and Ponader C. W. (1987) X-ray absorption study of the potassium coordination environment in glasses from the $NaAlSi_3O_8$-$KAlSi_3O_8$ binary: structural implications for the mixed-alkali effect. *J. Non-Cryst. Solids* **93,** 311–322.

Kotelnikov A. R. and Chernysheva I. V. (1995) Excess free energies of mixing of Sr,Ba-bearing binary feldspar solid solutions (experimental data). *Mineral. Mag.* **59,** 79–91.

Yund R. A. (1983) Microstructure, kinetics and mechanisms of alkali feldspar exsolution. In *Feldspar Mineralogy* (ed. P. H. Ribbe), 2nd ed., pp. 177–202. Mineral. Soc. Amer.

Yund R. A. (1983) Diffusion in feldspars. In *Feldspar Mineralogy* (ed. P. H. Ribbe), 2nd ed., pp. 203–222. Mineral. Soc. Amer.